

# Marginalized Particle Filter for Sensorless Control of PMSM Drives

Václav Šmídl

Institute of Information Theory and Automation  
Prague, Czech Republic  
email: smidl@utia.cas.cz

Zdeněk Peroutka

Regional Innovation Centre for Electrical Engineering  
University of West Bohemia  
Pilsen, Czech Republic  
email: peroutka@ieee.org

**Abstract**—Marginalized particle filter is a stochastic filter combining Kalman filters with particle filters. It decomposes the model into linear and nonlinear part and applies the Kalman filter for the former and the particle filter for the latter. Its application in sensorless control of permanent magnet synchronous motor (PMSM) drives is based on separate treatment of the state variables: the rotor position is represented by a set of samples (particles), and the rotor speed is estimated by the Kalman filters associated with each sample. In effect, this allows to represent accurately the inherent non-Gaussianity and nonlinearity of the model. We show that the resulting filter is capable to estimate the rotor position in the full speed range, including the standstill. Analysis of the filter performance is presented on open-loop off-line analysis of data recorded on a drive prototype. Execution time of optimized implementation of the algorithm for six particles in DSP is comparable to that of the Extended Kalman filter for full state-space model. Closed-loop performance of the filter (a sensorless drive control) is evaluated on developed drive prototype of rated power of 10.7kW.

## I. INTRODUCTION

Sensorless control of an ac drive—i.e. its operation without either a rotor position and/or speed sensor—is divided into two main directions: model-based approach and anisotropy approach. The model-based approach ranges from MRAS [1], through neural networks [2] to the extended Kalman Filter (EKF) [3] and the unscented Kalman filter [4]. The anisotropy based approach is based on injecting high-frequency signals into the input stator voltage and evaluation of their response using stator current of the drive [5]. The model based approaches are more reliable in the high speed regimes while the anisotropy based approach is superior in the low speed range and especially in the standstill. This is the reason for derivation of combined approaches [6] and switching schemes (often called hybrid estimators) [7].

Following the analysis of the extended Kalman filter [8], we conjecture that the reason why contemporary model-based approaches can not perform well in zero speed is their incapability to handle non-Gaussian distributions that arise in standstill of the drive. Therefore, we seek an estimation method that is capable to handle them. The most general methods for estimation of non-linear non-Gaussian systems are the sequential Monte Carlo methods, also known as the particle filters [9]. However, their computational demands are prohibitive on common hardware used for control of ac motor drives. In this paper, we assume Gaussian distributed errors on

the state-space model, however we represent unknown position of the rotor by an empirical distribution. Such a system is ready to be estimated by the marginalized particle filter, [10], also known as the Rao-Blackwellized particle filter [9].

## II. MATHEMATICAL MODEL OF PMSM

A commonly used model of a PMSM is mathematical model in rotating reference frame linked to a rotor flux linkage vector discretized by simple first-order Euler formula for time step  $\Delta t$ :

$$i_{d,t+1} = a_d i_{d,t} + b_d i_{q,t} \omega_t + c_d u_{d,t} + \epsilon_{d,t}, \quad (1)$$

$$i_{q,t+1} = a_q i_{q,t} - f_q \omega_t - b_q i_{d,t} \omega_t + c_q u_{q,t} + \epsilon_{q,t}, \quad (2)$$

$$\omega_{me,t+1} = \omega_{me,t} + \epsilon_{\omega,t}, \quad (3)$$

$$\vartheta_{e,t+1} = \vartheta_{e,t} + \omega_{me,t} \Delta t + \epsilon_{\vartheta,t}. \quad (4)$$

Here,  $i_d$ ,  $i_q$ ,  $u_d$  and  $u_q$  represent components of stator current and voltage vector in the rotating reference frame, respectively;  $\omega_{me}$  is electrical rotor speed and  $\vartheta_e$  is electrical rotor position. Constants  $a_d = (1 - \frac{R_s}{L_{sd}} \Delta t)$ ,  $a_q = (1 - \frac{R_s}{L_{sq}} \Delta t)$  differ in the used stator inductance  $L_{sd}$  and  $L_{sq}$ , respectively, so do  $b_d = \frac{L_{sq}}{L_{sd}} \Delta t$ ,  $b_q = \frac{L_{sd}}{L_{sq}} \Delta t$ ,  $c_d = \frac{\Delta t}{L_{sd}}$  and  $c_q = \frac{\Delta t}{L_{sq}}$ ;  $R_s$  is a stator resistance.  $f_q = \frac{\Psi_{pm}}{L_{sq}} \Delta t$ , where  $\Psi_{pm}$  is the flux linkage excited by permanent magnets on the rotor, and  $\Delta t$  is the sampling period. Simplified equation (3) considers “high” moment of inertia which means that we assume that the mechanical time constant is much longer than the sampling period (this assumption is fulfilled in many applications). Noise terms  $\epsilon_{d,t}$ ,  $\epsilon_{q,t}$ ,  $\epsilon_{\omega,t}$ ,  $\epsilon_{\vartheta,t}$ , aggregate errors caused by inaccurate discretization, uncertainties in parameters (e.g. due to temperature changes, saturation), unobserved physical effects (such as the unknown load, dead-time effects, non-linear voltage drops on power electronics devices).

Equations (1)–(4) represent non-linear state-space model of PMSM with state vector  $x_t = [i_{d,t}, i_{q,t}, \omega_{me,t}, \vartheta_{e,t}]$ . Traditionally all noise terms  $\epsilon$  were assumed to be Gaussian distributed to achieve consistency with the extended Kalman filter assumptions. Generally it is assumed that the noise between the state variables is uncorrelated and its variance is constant,  $Q = \text{diag}(q_i, q_i, q_\omega, q_\vartheta)$ .

In sensorless control it is assumed that only two state variables,  $i_{\alpha,t}$  and  $i_{\beta,t}$  are measured via observations  $\bar{i}_{\alpha,t}$  and

$\bar{i}_{\beta,t}$ , that are transformed into the rotating reference frame as follows:

$$\bar{i}_{d,t} = \bar{i}_{\alpha,t} \cos \vartheta_{e,t} + \bar{i}_{\beta,t} \sin \vartheta_{e,t} + \bar{\epsilon}_{d,t}, \quad (5)$$

$$\bar{i}_{q,t} = -\bar{i}_{\alpha,t} \sin \vartheta_{e,t} + \bar{i}_{\beta,t} \cos \vartheta_{e,t} + \bar{\epsilon}_{q,t}. \quad (6)$$

The measurement errors are assumed to be non-correlated Gaussian with variances  $\text{var}(\bar{\epsilon}_{d,t}) = r_i$ ,  $\text{var}(\bar{\epsilon}_{q,t}) = r_i$ .

#### A. Reduced order model

Model (1)-(4) is a proper state-space model of the drive, however its evaluation may be too computationally demanding. Computational requirements motivate research of models with reduced dimension of the state, [11]. Following [12], we consider only the electrical speed and rotor position to be the state variables  $x_t = [\omega_{me,t}, \vartheta_{e,t}]$  with state evolution equations (3)–(4). A minor drawback of this formulation is that the current observations  $\bar{i}_{d,t}$  and  $\bar{i}_{q,t}$  are informative only about  $\omega_{me,t-1}$  and  $\vartheta_{e,t-1}$ . In effect, the model allows to estimate only delayed values of the state. However, the current state estimates can be well approximated by predicted values  $x_t$  obtained by (3)–(4).

#### B. Non-Gaussian model

Application of the EKF (and also UKF) is based on two assumptions: (i) the noise distributions  $\epsilon$  are Gaussian, and (ii) the estimates of the unknown state are represented by their mean value and variance. The first assumption can be justified by a conservative choice of the noise variance. The second assumption is however problematic for the following reasons:

- 1) The rotor position is restricted to  $\langle -\pi, \pi \rangle$ , contradicting the Gaussian assumption of infinite support.
- 2) Expected value of  $\vartheta_e$  for a Gaussian distribution is always on the unit circle.
- 3) For any state values  $\omega_{me,t}, \vartheta_e$  the inverse values  $-\omega_{me,t}, \vartheta_e + \pi$  yields very similar output (5)–(6) in low speed region. These two modes are hard to distinguish and a Gaussian estimator must choose one of them without sufficient information.

The first two issues can be resolved using truncation of the Gaussian on the interval  $\langle -\pi, \pi \rangle$ , and the third by using a mixture of Gaussian. However, such extensions increase complexity of the estimation algorithms. Therefore, we seek a representation of estimates that allows non-conflicting description of the state uncertainty.

### III. MARGINALIZED PARTICLE FILTERING

Marginalized particle filtering is a technique of Bayesian filtering, where all unknowns are represented by probability density functions (distributions). By *Bayesian Filtering* we mean the recursive evaluation of the filtering distribution,  $p(x_t|y_{1:t})$ , using Bayes rule:

$$p(x_t|y_{1:t}) = \frac{p(y_t|x_t)p(x_t|y_{1:t-1})}{p(y_t|y_{1:t-1})}, \quad (7)$$

$$p(x_t|y_{1:t-1}) = \int p(x_t|x_{t-1})p(x_{t-1}|y_{1:t-1})dx_{t-1}, \quad (8)$$

where  $p(x_1|y_0)$  is the prior distribution, and  $y_{1:t} = [y_1, \dots, y_t]$  denotes the set of all observations.

Equations (7)–(8) are analytically tractable only for a limited set of models. The most notable example of an analytically tractable model is linear Gaussian for which (7)–(8) are equivalent to the Kalman filter. For other models, (7)–(8) need to be evaluated approximately.

#### A. Particle filtering

The particle filtering is based on approximation of the posterior (7) by an empirical probability density function

$$p(x_{1:t}|y_{1:t}) \approx \sum_{i=1}^N w_t^{(i)} \delta(x_{1:t} - x_{1:t}^{(i)}), \quad (9)$$

where  $x_{1:t}^{(i)}$ ,  $i = 1, \dots, N$ , are samples of the state space trajectory. Assimilation of the measured data is then achieved via sampling-importance-resampling procedure, where the weights can be computed recursively,

$$w_t^{(i)} \propto w_{t-1}^{(i)} \frac{p(y_t|x_t)p(x_t|x_{t-1})}{q(x_t|y_t)}. \quad (10)$$

Good proposal function and resampling strategy are necessary steps preventing degeneracy of the particle filter (10), [9].

The main advantage of this approach is its ability to approximate the filtering problem for non-linear non-Gaussian systems with an arbitrary accuracy. The main disadvantage is that for complex problems, the number of particles  $N$  has to be rather large to achieve good results.

#### B. Marginalized particle filtering (MPF) theory

Approximation (9) is unnecessary if the system has a linear Gaussian part [10]. In such a case, it is possible to split the state into linear and non-linear part,  $x_t = [x_t^l, x_t^n]$ , such that

$$x_{t+1}^l = A(x_t^n)x_t^l + B(x_t^n)u_t + \epsilon_{l,t}, \quad (11)$$

$$x_{t+1}^n = f(x_t, u_t, \epsilon_{n,t}), \quad (12)$$

$$y_t = C(x_t^n)x_t^l + Du_t + \epsilon_{y,t}. \quad (13)$$

Here,  $\epsilon_{l,t}$  and  $\epsilon_{y,t}$  are assumed to be Gaussian-distributed with zero mean known covariance matrix. Function  $f()$  is an arbitrary non-linearity and  $\epsilon_{n,t}$  can have an arbitrary distribution. Note that if  $x_t^n$  was known, equations (11) and (13) form a linear Gaussian model that can be estimated by the Kalman filter. The resulting estimate would be in the form of Gaussian density with mean and covariance dependent on the (known) non-linear state.

The idea of the MPF is to approximate the posterior density of the non-linear part by the empirical density (9). The full posterior density is then approximated by the chain rule of probability calculus as follows:

$$\begin{aligned} p(x_t^l, x_t^n|y_{1:t}) &= p(x_t^l|x_{1:t}^n, y_{1:t})p(x_t^n|y_{1:t}), \\ &= \sum_{i=1}^n w_t^{(i)} \mathcal{N}(\hat{x}_t^{l(i)}, P_t^{(i)}) \delta(x_t^{n(i)} - x_t^n). \end{aligned}$$

Here,  $x_t^{n(i)}$ ,  $i = 1, \dots, n$ , are the samples from the non-linear state and  $\mathcal{N}(\hat{x}_t^{l(i)}, P_t^{(i)})$  is the posterior density of the  $i$ th

**Initialize:** generate  $\omega_0^{(i)}, \vartheta_0^{(i)}$  and set  $w_0^{(i)} = 1/N$ .

**On-line:** At each time step:

- 1) For each particle:
  - a) Generate new  $\vartheta_t^{(i)}$  using (4), and compute d-q transformation (5)–(6),
  - b) Execute the Kalman filter (14)–(15) to obtain  $\omega_t^{(i)}, P_t^{(i)}$  and  $p(y_t|y_{1:t-1}, \vartheta_{me}^{(i)})$ ,
- 2) Evaluate weights  $w_t$  (16),
- 3) Resample the particles using deterministic resampling.

Figure 1. Algorithm of the MPF for the reduced order model of the PMSM drive.

Kalman filter associated with the  $i$ th particle of the non-linear state.

### C. MPF for the PMSM drive

We note that for a known value of  $\vartheta_{e,t}$ , the state variable in the PMSM model is  $\omega_{me,t}$ , with state evolution model (3) and observation equations (1)–(2). The model is consistent with form (11)–(13) under assignments:

$$\begin{aligned} A &= 1, \\ B &= 0, \\ y_t &= [i_{d,t} - a_d i_{d,t-1} - c_d u_{d,t-1}, \\ &\quad i_{q,t} - a_q i_{q,t-1} - c_q u_{q,t-1}]^T, \\ C &= [b_d i_{q,t}, -(f_q + b_q i_{d,t})]^T, \\ D &= [0, 0] \end{aligned}$$

Applying the standard Kalman filter equations to the system above, we obtain equations for estimates of the rotor speed for a given particle of the rotor position  $\vartheta_{e,t}^{(i)}$  as follows:

$$\begin{aligned} \hat{\omega}_{me,t}^{(i)} &= \hat{\omega}_{me,t-1}^{(i)} + K^{(i)} \left( y_t - C^{(i)} \hat{\omega}_{me,t-1}^{(i)} \right), \quad (14) \\ K^{(i)} &= P_{t-1}^{(i)} C^{(i)T} \rho^{(i)}, \\ \rho^{(i)} &= \frac{1}{r} \left( 1 - \zeta^{(i)} C^{(i)T} C^{(i)} \right). \\ \zeta^{(i)} &= \frac{P_{t-1}^{(i)}}{r + P_{t-1}^{(i)} C^{(i)T} C^{(i)}}. \\ P_t^{(i)} &= P_{t-1}^{(i)} \left( 1 - K^{(i)} C^{(i)} \right) + q_\omega. \quad (15) \end{aligned}$$

Each of these filters has associated weight

$$w_t^{(i)} \propto p(y_t, \omega_{me}|y_{1:t-1}, \vartheta_{e,t}^{(i)}) w_{t-1}^{(i)}, \quad (16)$$

assuming that the transition density was used as the proposal. The predictive likelihood needed in (16) is computed as:

$$p(y_t|y_{1:t-1}, \vartheta_{e,t}^{(i)}) \propto \sqrt{\frac{\rho}{r}} \exp \left( -\frac{1}{2} (y - \hat{y})' \left( \frac{1}{r} (I - \zeta C C') \right) (y - \hat{y}) \right) \quad (17)$$

The final MPF algorithm for the PMSM drive is summarized in Figure 1.

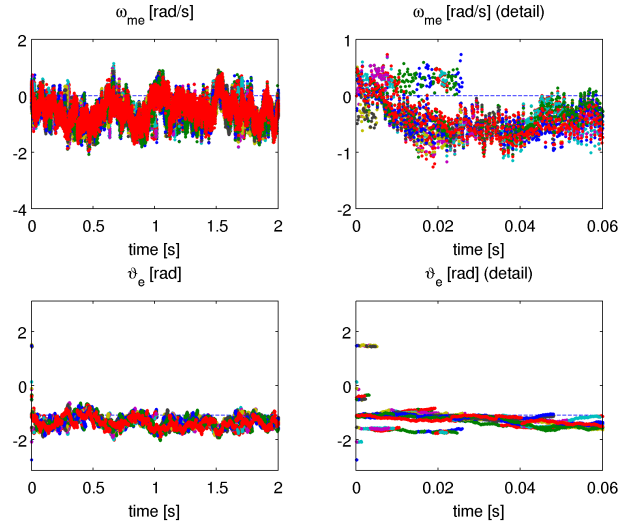


Figure 2. State estimation in open-loop using MPF with  $N = 10$  and recorded data at  $\omega_{me} = 0$  rad/s (standstill, locked rotor). Dashed line denotes observed values from shaft sensors.

## IV. OPEN-LOOP VALIDATION OF PROPOSED MPF

Open-loop analysis of the MPF filter was performed off-line on a PC using data recorded on a running drive of rated power of 10.7kW operated in sensed mode. This allows us to tune model parameters and algorithm simplification that are necessary for efficient implementation.

### A. Parameter identification

Parameters of the drive were identified using recursive least squares approach. The parameters of the drive were identified to be:

$$\begin{aligned} a_d &= 0.98, & a_q &= 0.99, \\ b_d &= 0.00013, & b_q &= 0.00011, \\ c_d &= 0.040, & c_q &= 0.036, \\ & & f_q &= 0.0083, \end{aligned} \quad (18)$$

However, it was observed that the parameters vary with operating point of the motor. Parameter values listed in (18) were chosen as a compromise for overall performance.

### B. Standstill operation

Data recorded in standstill were measured under locked rotor to guarantee that the rotor is not moving. For better identifiability, the input stator voltage was injected with square signal of frequency 500Hz. Position of the drive was estimated using the MPF algorithm with 10 particles and covariance matrices  $q_\omega = 0.1, q_\vartheta = 0.01, r = 0.05$ . Results of estimation are displayed in Fig. 2 via position of all particles for the rotor position (bottom row) and mean values of all Kalman filters for the rotor speed (top row). The particles are initialized by random draw of  $\vartheta_e^{(i)}$  from uniform distribution on interval  $\langle -\pi, \pi \rangle$ , the prior estimate of rotor speed is  $\hat{\omega}_{me} = 0, P_0 = 1$ .

For better understanding of the principle, the first 0.06 seconds of the part of the estimation is displayed in the right

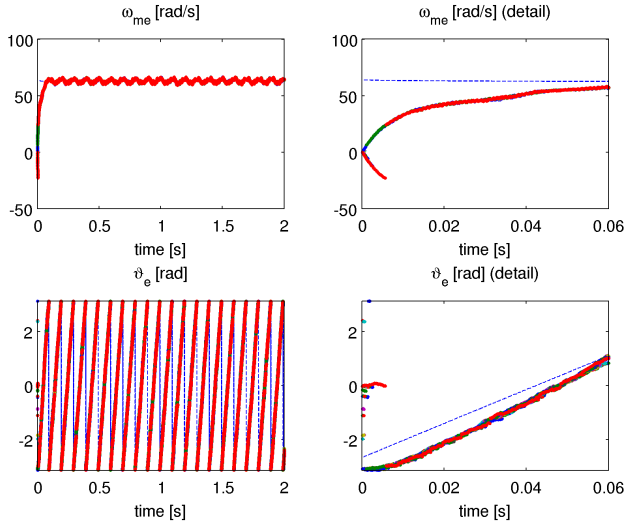


Figure 3. State estimation in open-loop using MPF with  $N = 10$  and recorded data at fixed electrical rotor speed of  $\omega_{me} = 62$  rad/s. Dashed line denotes measured values of the state variables from sensors.

column of Fig. 2. Note on the detail of the rotor position, that the particles evolve from the initial positions by random walk forming a typical random walk paths. Thickness of the paths is given by the number of particles associated with the track. The track ends when the associated particle weights are so small that the resampling operation does not copy the particle to the next step. After circa 0.04s, all particles are concentrated around the observed value. The second longest track in the detail view of the position is around the second mode of solution at  $[\vartheta_e + \pi, -\omega_{me}]$  (Section II-B). Occasionally, for different realization of the particles, this second mode becomes dominant and all particles concentrate around it. This problem is also known in the traditional hf signal injection methods.

### C. Constant rotor speed

The same experiment was performed with data recorded on the drive prototype running at fixed electrical rotor speed of  $\omega_{me} = 62$  rad/s. The number of particles and the initial conditions were the same as those in Section IV-B. Results of estimation are displayed in Fig. 3 via particles  $\vartheta_e^{(i)}$  and mean values of the associated Kalman filters  $\hat{\omega}_{me}^{(i)}$ . Note that even though the initial conditions are far from the true value, the filter is able to reach the true value within 0.06s. The second mode of solution is also visible, however, in this case, it is reliably removed after less than 0.01 second.

## V. SENSORLESS CONTROL OF PMSM DRIVE

### A. Implementation of MPF

Since the output of the MPF is in the form of probability distribution, we need to find an estimate for the control design. In representation (9), the expected value of  $\vartheta_e$  does not have

a good meaning. Therefore, we use

$$\hat{\vartheta}_{e,t} = \arctan \frac{\sum_{i=1}^N w_t^{(i)} \sin \vartheta_e^{(i)}}{\sum_{i=1}^N w_t^{(i)} \cos \vartheta_e^{(i)}}, \quad (19)$$

$$\hat{\omega}_{me,t} = \sum_{i=1}^N w_t^{(i)} \omega_t^{(i)}. \quad (20)$$

These estimates are inputs to the employed conventional vector control algorithm of the drive described in more details in the following section.

### B. Drive Control Under Tests

Configuration of the investigated sensorless drive control is displayed in Fig. 4. The drive control is based on the conventional vector control in Cartesian coordinates in rotating reference frame (d,q) linked to a rotor flux linkage vector. An input to the drive controller is the commanded electrical rotor speed  $\omega_{mew}$  which is controlled by the PI controller  $R_\omega$ . Output of  $R_\omega$  is the demanded torque component  $I_{sqw}$  of the stator current vector. The torque ( $I_{sqw}$ ) and flux ( $I_{sdw}$ ) currents are controlled by the PI controllers  $R_{Isd}$  and  $R_{Isq}$ , respectively. The flux weakening is secured by the PI controller  $R_{U_{rm}}$  which controls the PWM modulation depth (signal  $U_{rm}$ ) and commands the flux current  $I_{sdw}$ . The current controllers are supported by block “voltage calculation” (often referred to as “decoupling”) which computes the components of the required stator voltage vector in (d,q) frame using a simplified model of the PMSM in steady-state. The components of the stator current vector ( $i_{s\alpha}, i_{s\beta}$ ) and the reconstructed stator voltage vector  $u_{s\alpha}, u_{s\beta}$  in the stationary reference frame are inputs to the MPF. The stator voltage vector is reconstructed from the measured dc-link voltage and known switching combination of the voltage-source converter. The MPF output is the estimated electrical rotor speed  $\hat{\omega}_{me}$  and the electrical rotor position  $\hat{\vartheta}_e$ . The drive can be operated in two modes: (i) sensed mode (where the drive control uses the rotor speed and position from the rotor position sensor and the MPF is operated in open-loop), and (ii) sensorless mode (where drive control uses the MPF output and hence, MPF is operated in closed-loop). The voltage-source converter employs a third-harmonic injected PWM with carrier frequency of 4kHz. The sampling frequency of the MPF as well as of the drive control has been set to 125μs.

The covariance matrices of all tested variants of MPF were considered to be time- and state-invariant and were obtained by manual tuning. The proposed sensorless drive control with presented algorithm of the MPF (Fig. 4) has been tested on a developed prototype of PMSM drive of rated power of 10.7kW.

## VI. EXPERIMENTAL RESULTS

The developed prototype of a PMSM drive was during the experimental tests operated in both sensed and sensorless mode. All results are obtained with MPF with 5 particles and covariance matrices  $q_\omega = 0.1$ ,  $q_\vartheta = 0.003$ ,  $r = 0.05$ . Execution time of this MPF configuration on the TI



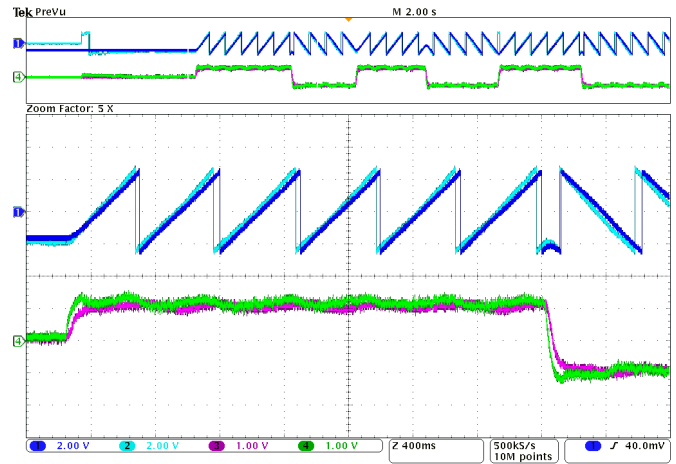
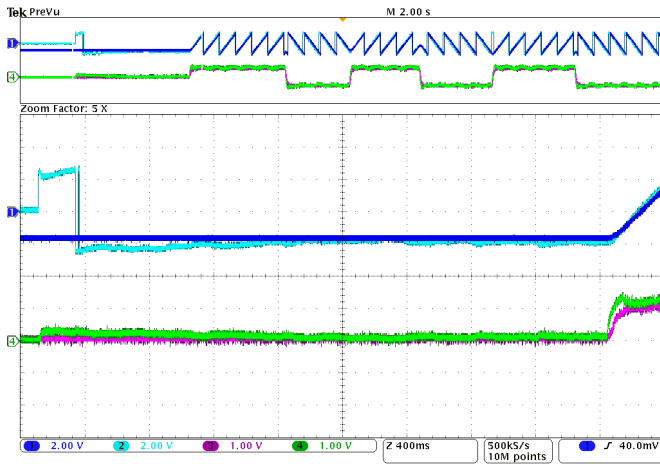


Figure 5. Experimental result – sensed mode of the drive control (MPF operated in open-loop): Initial rotor position and speed estimation and step changes of commanded mechanical rotor speed of  $\pm 30$  rpm. Detail of initial rotor position and speed estimation (left) and acceleration from standstill to 30 rpm and speed reversal to -30 rpm (right). **ch1**: electrical rotor position (sensor) [144 deg/div], **ch2**: estimated electrical rotor position (MPF) [144 deg/div], **ch3**: rotor speed (sensor) [30 rpm/div], **ch4**: estimated rotor speed (MPF) [30 rpm/div], time scale: 400 ms/div

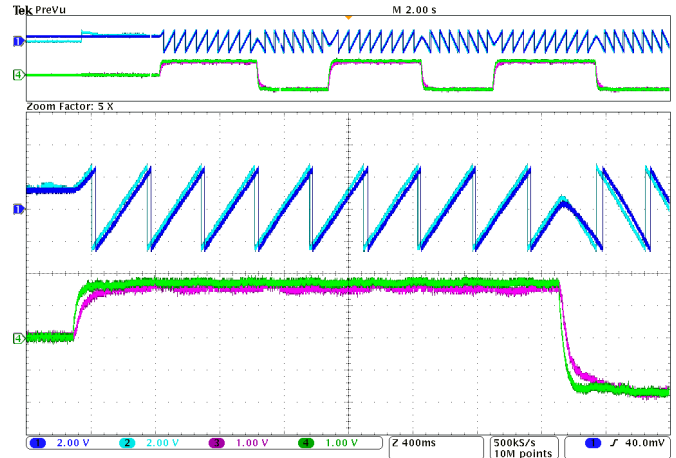
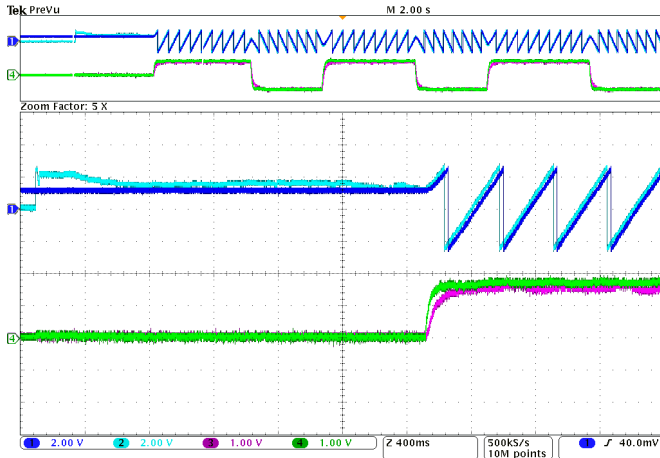


Figure 6. Experimental result – sensorless mode of the drive control: Initial rotor position and speed estimation and step changes of commanded mechanical rotor speed of  $\pm 50$  rpm. Detail of initial rotor position and speed estimation (left) and acceleration from standstill to 50 rpm and speed reversal to -50 rpm (right). **ch1**: electrical rotor position (sensor) [144 deg/div], **ch2**: estimated electrical rotor position (MPF) [144 deg/div], **ch3**: rotor speed (sensor) [30 rpm/div], **ch4**: estimated rotor speed (MPF) [30 rpm/div], time scale: 400 ms/div

## REFERENCES

- [1] T. Orlowska-Kowalska and M. Dybkowski, "Stator-current-based mras estimator for a wide range speed-sensorless induction-motor drive," *Industrial Electronics, IEEE Trans. on*, vol. 57, no. 4, pp. 1296–1308, 2010.
- [2] P. Brandstetter, M. Kuchar, and D. Vinklerek, "Estimation techniques for sensorless speed control of induction motor drive," in *Industrial Electronics, 2006 IEEE International Symposium on*, vol. 1, pp. 154–159, July 2006.
- [3] R. Dhaouadi, N. Mohan, and L. Norum, "Design and implementation of an extended Kalman filter for the state estimation of a permanent magnet synchronous motor," *Power Electronics, IEEE Transactions on*, vol. 6, no. 3, pp. 491–497, 1991.
- [4] B. Akin, U. Orguner, A. Ersak, and M. Ehsani, "Simple derivative-free nonlinear state observer for sensorless ac drives," *Mechatronics, IEEE/ASME Transactions on*, vol. 11, pp. 634–643, Oct. 2006.
- [5] J. Holtz, "Sensorless position control of induction motors—an emerging technology," *Industrial Electronics, IEEE Trans. on*, vol. 45, pp. 840–851, Dec. 1998.
- [6] F. Abry, A. Zgorski, X. Lin-Shi, and J.-M. Retif, "Sensorless position control for spmsm at zero speed and acceleration," in *Power Electronics and Applications (EPE 2011), Proceedings of the 2011-14th European Conference on*, pp. 1–9, 30 2011-sept. 1 2011.
- [7] D. Vosmik and Z. Peroutka, "Sensorless control of permanent magnet synchronous motor employing extended kalman filter in combination with hf injection method," in *Power Electronics and Applications (EPE 2011), Proceedings of the 2011-14th European Conference on*, pp. 1–10, 30 2011-sept. 1 2011.
- [8] Z. Peroutka, V. Šmídl, and D. Vošmik, "Challenges and limits of extended kalman filter based sensorless control of permanent magnet synchronous machine drives," in *Proc. of the 13th European Conference on Power Electronics and Applications*, (Barcelona, Spain), 2009.
- [9] A. Doucet, N. de Freitas, and N. Gordon, eds., *Sequential Monte Carlo Methods in Practice*. Springer, 2001.
- [10] T. Schön, F. Gustafsson, and P.-J. Nordlund, "Marginalized particle filters for mixed linear/nonlinear state-space models," *IEEE Transactions on Signal Processing*, vol. 53, pp. 2279–2289, 2005.
- [11] J. Kim and S. Sul, "High performance PMSM drives without rotational position sensors using reduced order observer," in *Industry Applications Conference, 1995. Thirtieth IAS Annual Meeting, IAS'95., Conference Record of the 1995 IEEE*, vol. 1, pp. 75–82, IEEE, 1995.
- [12] V. Šmídl and Z. Peroutka, "Reduced-order square-root ekf for sensorless control of pmsm drives," in *Proc. of the 37th Annual Conference of the IEEE Industrial Electronics Society*, (Melbourne, Australia), 2011.